JACS
JOURNAL OF THE AMERICAN CHEMICAL SOCIETY
Communication
pubs.acs.org/JACS

Multipoint Interactions Enhanced CO_2 Uptake: A Zeolite-like Zinc–Tetrazole Framework with 24-Nuclear Zinc Cages

Ping Cui,[†] Yu-Guang Ma,[§] Huan-Huan Li,[†] Bin Zhao,*[,†] Jian-Rong Li,[‡] Peng Cheng,[†] Perla B. Balbuena,*[,§] and Hong-Cai Zhou[‡]

[†]Department of Chemistry, Key Laboratory of Advanced Energy Material Chemistry, MOE, and TKL of Metal and Molecule Based Material Chemistry, Nankai University, Tianjin 300071, China

[‡]Department of Chemistry and [§]Department of Chemical Engineering, Texas A&M University, College Station, Texas 77842, United States

Supporting Information

ABSTRACT: A zeolite-like microporous tetrazole-based metal–organic framework (MOF) with 24 nuclear zinc cages was synthesized and characterized. It exhibits high CO_2 adsorption capacity up to 35.6 wt % (8.09 mmol/g) and excellent CO_2/CH_4 selectivity at 273 K/1 bar, being among the highest values known to date. Theoretical calculations based on simulated annealing techniques and periodic DFT revealed that CO_2 is predominantly located around the inner surface of the cages through multipoint interactions, in particular, around the aromatic tetrazole rings. Importantly, it is the first time that multipoint interactions between CO_2 molecules and frameworks resulting in high CO_2 uptake are observed.

Metal–organic frameworks (MOFs), a subclass of porous materials with high thermal and chemical stabilities, high surface areas, and chemical tenability, are particularly attractive synthetic targets due to their fundamental interest and potential applications in clean energy, sensors, catalysis, etc.[1−3] Among them, CO_2 capture is considered a promising strategy to cope with environmental problems stemming from greenhouse effects.[4] Therefore, CO_2 capture from flue streams and natural and fuel gases, involving CO_2/N_2, CO_2/CH_4, and CO_2/H_2 separation, respectively, through MOFs, has been highly investigated in recent years.[5] To enhance CO_2 adsorption capacity and selectivity, various strategies have been explored in MOFs construction, including control of pore size,[6] adjustment of surface area and pore volume,[7] and functionalization of MOFs by introducing functional groups[8] and generating exposed framework atoms (e.g., open metal[9] and donor sites[10]). To date, under 273 K/1 bar conditions, the highest CO_2 uptake of 40.5 wt % (9.2 mmol/g) was observed in a microporous copper-based MOF [Cu(Me-4py-trz-ia)].[11] Although great progress in gas storage capacity and adsorption selectivity of MOFs has been made, seeking new strategies to further improve gas storage capacity of MOF materials is still a great challenge.

Multifold weak interactions among one molecule and several sites on a biological cell surface, namely, multipoint interactions, may drastically reinforce the binding energy between molecule and cell, existing extensively in the cell and playing a crucial role in various physiological functions.[12] By such analogy, multipoint interactions could effectively enhance CO_2 adsorption capacity of MOFs when they exist among adsorbed CO_2 molecules and the wall surface of channels in microporous MOFs. To confirma, we selected a flexible tetrazole derivative ligand, 1,5-bis(5-tetrazolo)-3-oxapentane (H_2btz in Scheme S1) as the organic linker to construct porous MOFs, where multipoint interactions may theoretically exist between CO_2 and frameworks: (1) π-electron system of aromatic tetrazole rings and C atom of CO_2; (2) potential exposed nitrogen atoms from tetrazole rings and C atom of CO_2; (3) O atoms of CO_2 and C–H bonds of O-$(CH_2CH_2-)_2$ moiety in H_2btz.

Based on the H_2btz ligand, we present a novel microporous tetrazole-based MOF with a sodalite (sod) topology (Figure 1),

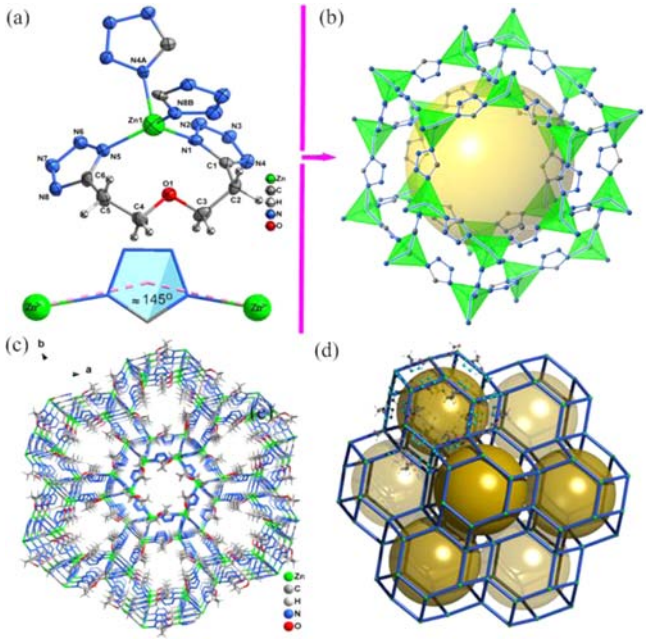

Figure 1. (a) Zn^{2+} ion coordination environment and Tz ring coordination mode. (b) Zn24 cage in **1**. (c) Perspective view of the framework structure of **1**. (d) The sod topological net of **1**.

Received: June 28, 2012
Published: October 31, 2012

   dx.doi.org/10.1021/ja3063138 | J. Am. Chem. Soc. 2012, 134, 18892–18895

$\{[Zn(btz)]\cdot DMF\cdot 0.5H_2O\}_n$ (**1**, H_2btz = 1,5-bis(5-tetrazolo)-3-oxapentane, DMF = *N*,*N*′-dimethylformamide), and to the best of our knowledge, this zeolite-like MOF (ZMOF) based on the tetrazolate (Tz) ligands is among rarely documented examples.[13] CO_2 adsorption capacity and CO_2/CH_4 selectivity of its desolvated phase **1b** are 35.6 wt % (8.1 mmol/g) and 21.1 at 273K/1 bar, which are among the highest known for MOFs.[4,11] This excellent adsorption capacity and separation performance can be attributed to multipoint interactions between CO_2 molecules and adsorbent, providing new insight for the design of MOFs for gas storage and separation.

Single crystals of **1** were prepared by reaction of $Zn(NO_3)_2\cdot 6H_2O$ with H_2btz in a DMF and methanol mixture at rt (see the Supporting Information, SI). **1** crystallizes in the trigonal space group *R*-3, with one crystallographically independent Zn^{2+} ion and one ligand anion in the asymmetric unit (Figure 1a). The tetrahedral Zn^{2+} center is coordinated by four nitrogen atoms from Tz rings. In addition, there is a weak coordination between the oxygen atom of btz^{2-} ligand and the Zn^{2+} center with Zn···O distance of 2.7 Å. Each Tz ring is attached to two Zn^{2+} ions in μ_2-bridged fashion with coordination angle of ∼145° (Zn−Tz−Zn), analogous to imidazolate rings in zeolite−imidazolate frameworks (ZIFs).[14] Through these connection modes, 24 Zn(II) ions and 36 Tz rings stitch into a 24 nuclear zinc sod cage with a ∼7.2 Å diameter cavity (Figures 1b and S1), exhibiting truncated octahedral geometry with eight hexagonal windows (two regular, six twisted) on its surface. The regular window of the cage is 6.34 × 6.34 $Å^2$ (atom to atom distance). The cage as a repeat unit is further extended into microporous zeolite-like 3D framework with sod topology (Figures 1c,d and S2). Upon removal of guest molecules, the structure of **1** has a porosity of ∼45.6%, calculated with PLATON software.[15]

TGA of **1** indicated that guest water molecules were lost <100 °C with weight loss of 2.6% (calcd 2.5%), then followed by DMF molecule loss (obsd, 20.4%; calcd, 20.5%). Framework of **1** began to gradually decompose >300 °C (Figure S3). **1a** (CH_2Cl_2 exchanged sample **1**) and **1b** (CH_2Cl_2 removed **1a** under vacuum at 60 °C) TGA results reveal negligible weight loss before 350 °C, suggesting that guest molecules in **1** can be effectively removed by solvent exchange strategy. Importantly, investigation on powder X-ray diffraction patterns demonstrated that porous frameworks of **1** still retain their integrity even after removal of guest molecules and/or gas adsorption (Figure S4).

To confirm porosity of activated material **1b**, the sorption isotherm of Ar was conducted and analyzed. The Ar sorption (87 K) of **1b** shows a fully reversible like-I isotherm (Figure S6), characteristic of permanent microporous materials. The apparent Brunauer−Emmett−Teller (BET) and Langmuir surface areas are estimated to be 1151 and 1222 m^2/g, respectively. Nonlocal DFT analysis on the isotherm data shows that pore size is ∼5.5 Å in diameter (Figure S7). Additionally, total pore volume calculated from Ar adsorption isotherm is 0.65 cm^3/g.

H_2 sorption isotherms of **1b** were measured at 77 and 87 K, as shown in Figures 2 and S8. Shape of the isotherms indicates that H_2 sorption is reversibly physisorption. H_2 sorption capability (P/P_o = 1.0) is up to 11.39 mmol g^{-1} (2.28 wt %) at 77 K, which is significantly higher than several other porous ZMOFs (ZIF-20, 1.1 wt %; *ρ*-ZMOF, 1.16 wt %; ZIF-8, 1.27 wt %; ZIF-11, 1.35 wt %).[16] Isosteric heat (Q_{st}) of H_2 sorption is estimated to be 8.1 kJ/mol at zero coverage (Figure S9), which is moderate compared with other porous materials.[1d]

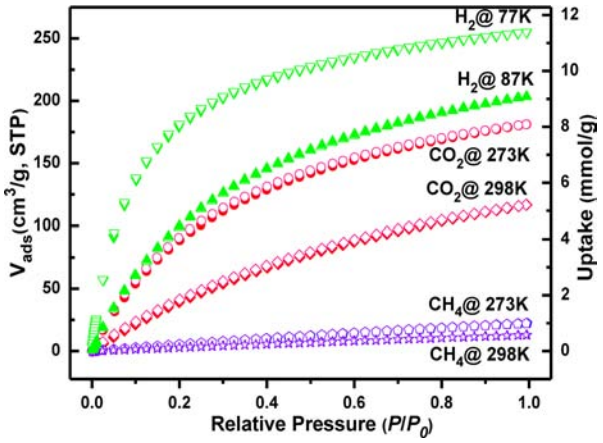

Figure 2. H_2, CH_4, and CO_2 sorption isotherms. STP = standard temperature and pressure.

Sorption behaviors of **1b** toward CH_4 and CO_2 were studied at 273 and 298 K (Figures 2 and S10−13). The amount of CH_4 uptake at 273 and 298 K (P/P_o = 1.0) is 0.99 (1.57) and 0.57 mmol/g (0.91 wt %), respectively. CH_4 sorption Q_{st} is estimated to be 19.6 kJ/mol at zero coverage (Figure S11). Interestingly, **1b** can adsorb a considerable amount of CO_2 at 273 K (P/P_o = 1.0) up to 8.09 mmol/g (35.6 wt %), corresponding to two CO_2 molecules per formula unit. At 298 K (P/P_o = 1.0), CO_2 uptake can still reach 4.99 mmol/g (21.96 wt %). CO_2 sorption Q_{st} of is 31.2 kJ/mol at zero coverage calculated from adsorption isotherms at 273 and 298K (Figure S13), which is slightly higher than the 30 kJ/mol in [Cu(Me-4py-trz-ia)] value.[11]

Particularly, features outlined above enable this new ZMOF to be a good gas separation candidate. Preliminary results (Figures S14 and S15) indicate that **1b** shows large adsorption selectivity of CO_2 over CH_4 with separation factor being 21.1 at 273 K and 1 bar.

To date, in reported zeolite-like MOFs and under the conditions of 273 K and 1 bar, the highest value (18.0 wt %) of adsorbing CO_2 was observed in IFMC-1 (Table 1), but the CO_2 adsorption (35.6 wt %) of **1b** presented in this work is almost two times as high as that of the former, setting a record. In addition, in all reported MOFs, only two samples exhibit higher adsorption amount of CO_2 than **1b** (Table 1). One is compound [Cu(Me-4py-trz-ia)] with the highest CO_2 adsorption of 40.5 wt %, and the other is SNU-5 with 38.5 wt % CO_2 adsorption. Interestingly, the BET surface area

Table 1. Comparison of High CO_2 Uptake Among MOFs, Zeolite-like MOFs and 1b at 273 K and 1 bar

material	CO_2 wt %	S_{BET} [m^2/g]	Q_{st} [kJ/mol]	functionality type
[Cu(Me-4py- trz-ia)][11]	40.5	1473	30	polar network
SNU-5[18]	38.5	2850	–[a]	exposed cations
1b, this work	35.6	1151	31.2	multipoint interactions
CAU-1[19]	24.1	1268	48	amines
IFMC-1[13c]	18.0	780	30.7	open N-donor sites

[a]No available data for Q_{st}.

dx.doi.org/10.1021/ja3063138 | J. Am. Chem. Soc. 2012, 134, 18892−18895

(S_{BET}) of **1b** is smaller than that of CAU-1, but its CO_2 adsorption amount is significantly higher than that of CAU-1; the S_{BET} of SNU-5 is about 2.5 times as large as that of **1b**, but the difference of CO_2 adsorption amount between them is very small. Furthermore, it was reported that high CO_2 adsorption maybe arises from exposed metal sites[9] or N donors,[10] network polarity,[11] or other factors,[4b] and the next logical problem is what causes the high adsorption behavior of **1b**. Besides, we also want to know why CO_2 adsorption of **1b** is higher than any reported of tetrazole-based MOFs.[13,17] According to all mentioned above, it is necessary to explore the mechanism of adsorbing CO_2 in **1b**.

The nature of the interactions between CO_2 molecules and the framework of **1** was studied by simulated annealing techniques and periodic DFT calculations (see the SI). CO_2 binding sites and corresponding heat of adsorption were obtained from the annealing simulations. The calculated value of Q_{st} is 33.8 kJ/mol, which is in good agreement with the experimental zero-loading Q_{st} (31.2 kJ/mol). The CO_2 sorption isotherms at 273 and 298 K show significant amounts of CO_2 uptake: ~40 molecules/unit cell (UC) at 273 K and ~25 molecules/UC at 298 K. As depicted in Figure 3, the CO_2 molecules are predominantly located around the inner surface of the cages, in particular, around the aromatic rings. A few CO_2 molecules are found in the cages center. To reveal the strong CO_2 adsorption origin, we examine two configurations with the largest (most negative) binding energies; corresponding geometries are illustrated in Figure 4. In configuration **A** (E_{bind} = −36.9 kJ/mol), the C atom in CO_2 shows several short contacts with N atoms in aromatic rings, while O atoms also have some close contacts with CH_2 groups, forming multipoint interactions. Similar phenomenon is also observed in configuration **B** (E_{bind} = −33.9 kJ/mol). These results strongly suggest that strong binding of CO_2 is contributed by multipoint interactions and possibly no major binding exists for CO_2 adsorption.

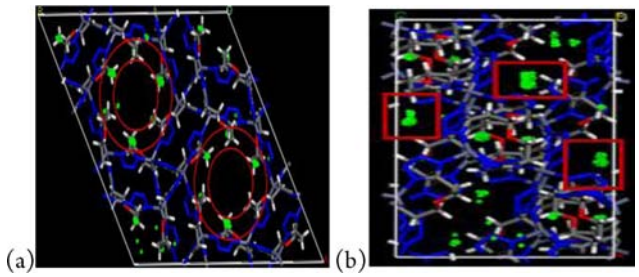

Figure 3. (a) Distribution of CO_2 adsorption sites, denoted as green points. Sites are predominately located between two circles. (b) Sites are close to the heterocyclic rings.

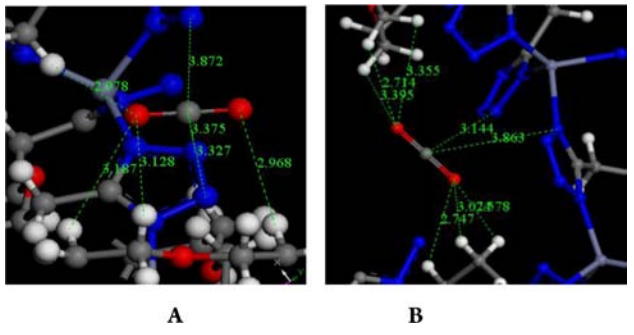

Figure 4. Preferred CO_2 adsorption site configurations by annealing simulations. Close contact distances, in Å, are marked.

To further understand CO_2 surface adsorption in MOF systems, we made geometry optimizations for the configurations **A** and **B** by using periodic DFT. Optimized geometries verify that CO_2 binding is stabilized by multipoint interactions (Figure 5). For example, the C atom in CO_2 molecule forms five close contacts with two aromatic rings (d_{C-N} = 3.42−3.88 Å) and one oxygen atom in the chain (d_{C-O} = 3.67 Å), while the O atom may shortly contact with six CH_2 groups (d_{O-H} = 2.94−3.45 Å) in configuration **A**. Calculated interaction energy is −13.4 and −9.7 kJ/mol for configurations **A** and **B**, respectively; values are much smaller than the experimental Q_{st}. The main reason is that the conventional GGA functional in DFT methods is unable to reproduce the van der Waals (vdW) interactions. (However, DFT can accurately evaluate Coulomb interactions.) As most of the interaction energy is missing in the DFT calculations, we can deduce that the major part of the binding energy is contributed by vdW (dispersion) interactions. To verify this, we performed DFT-D2 calculations in which a semiempirical dispersion potential was added.[20] The optimized geometries are similar to those from the conventional DFT method, with a slightly closer contact between CO_2 molecule and framework (Figure S16). The calculated interaction energy is much more negative, with −32.2 and −34.9 kJ/mol for configuration **A** and **B**, respectively, comparable to the experimental Q_{st}. This indicates that dispersion interactions dominate CO_2 adsorption in the framework, in good agreement with our deduction. Although a single vdW interaction is usually weak, the summation of the multi-weak interactions can produce a strong CO_2 binding to the MOF surface.

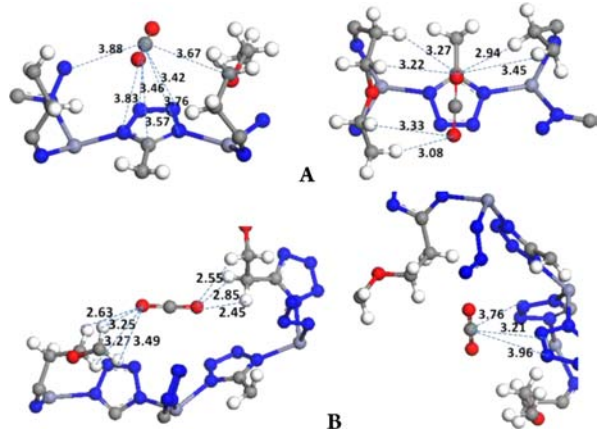

Figure 5. DFT optimized geometry for Figure 4 configurations. Close contact distances, in Å, are marked.

We also made a Bader charge analysis for the MOF systems (Figure S17). We found that two uncoordinated N atoms in the aromatic ring only carry slight negative charges (−0.06 and −0.09e). This might be why Coulomb interactions are not as strong as expected. Moreover, CO_2 adsorption does not lead to an obvious charge change for the MOF system atoms. The CO_2 molecule still remains electrically neutral, and there is no charge transfer for uncoordinated nitrogen atoms (Figure S17b and c). Therefore, CO_2 adsorption in the MOF is classified as physisorption, as expected.

dx.doi.org/10.1021/ja3063138 | J. Am. Chem. Soc. 2012, 134, 18892−18895

In summary, we have designed and synthesized a ZMOF showing high CO_2 adsorption capacity and large CO_2/CH_4 selectivity. An unprecedented multipoint interaction was proposed based on computational modeling and simulations, which may be a promising strategy to enhance gas adsorption capacity and separation performance of MOFs.

■ ASSOCIATED CONTENT

Supporting Information

Experimental details and characterization data. This material is available free of charge via the Internet at http://pubs.acs.org.

■ AUTHOR INFORMATION

Corresponding Author

zhaobin@nankai.edu.cn; balbuena@tamu.edu

Notes

The authors declare no competing financial interest.

■ ACKNOWLEDGMENTS

This work was supported by the 973 Program (grants 2012CB821702, 2011CB935902), NSFC (grants 20971074, 91122004), FANEDD (grant 200732), and NSF of Tianjin (Grant 10JCZDJC21700).

■ REFERENCES

(1) (a) Furukawa, H.; Yaghi, O. M. *J. Am. Chem. Soc.* **2009**, *131*, 8875. (b) Wu, H.; Zhou, W.; Yildirim, T. *J. Am. Chem. Soc.* **2009**, *131*, 4995. (c) Ma, S. Q.; Zhou, H. C. *Chem. Commun.* **2010**, *46*, 44. (d) Suh, M. P.; Park, H. J.; Prasad, T. K.; Lim, D. W. *Chem. Rev.* **2012**, *112*, 782.

(2) (a) Kreno, L. E.; Leong, K.; Farha, O. K.; Allendorf, M.; Van Duyne, R. P.; Hupp, J. T. *Chem. Rev.* **2012**, *112*, 1105. (b) Cui, Y. J.; Xu, H.; Yue, Y. F.; Guo, Z. Y.; Yu, J. C.; Chen, Z. X.; Gao, J. K.; Yang, Y.; Qian, G. D.; Chen, B. *J. Am. Chem. Soc.* **2012**, *134*, 3979.

(3) (a) Ma, L. Q.; Abney, C.; Lin, W. B. *Chem. Soc. Rev.* **2009**, *38*, 1248. (b) Ma, L. Q.; Falkowski, J. M.; Abney, C.; Lin, W. B. *Nat. Chem.* **2010**, *2*, 838. (c) Lu, G.; Li, S. Z.; Guo, Z.; Farha, O. K.; Hauser, B. G.; Qi, X. Y.; Wang, Y.; Wang, X.; Han, S. Y.; Liu, X. G.; DuChene, J. S.; Zhang, H.; Zhang, Q. C.; Chen, X. D.; Ma, J.; Loo, S. C. J.; Wei, W. D.; Yang, Y. H.; Hupp, J. T.; Huo, F. W. *Nat. Chem.* **2012**, *4*, 310.

(4) (a) Li, J. R.; Ma, Y. G.; McCarthy, M. C.; Sculley, J.; Yu, J. M.; Jeong, H. K.; Balbuena, P. B.; Zhou, H. C. *Coord. Chem. Rev.* **2011**, *255*, 1791. (b) Sumida, K.; Rogow, D. L.; Mason, J. A.; McDonald, T. M.; Bloch, E. D.; Herm, Z. R.; Bae, T. H.; Long, J. R. *Chem. Rev.* **2012**, *112*, 724.

(5) Li, J. R.; Sculley, J.; Zhou, H. C. *Chem. Rev.* **2012**, *112*, 869.

(6) (a) Farha, O. K; Malliakas, C. D.; Kanatzidis, M. G.; Hupp, J. T. *J. Am. Chem. Soc.* **2010**, *132*, 950. (b) An, J.; Rosi, N. L. *J. Am. Chem. Soc.* **2010**, *132*, 5578.

(7) Llewellyn, P. L.; Bourrelly, S.; Serre, C.; Vimont, A.; Daturi, M.; Hamon, L.; De Weireld, G.; Chang, J. S.; Hong, D. Y.; Hwang, Y. K.; Jhung, S. H.; Ferey, G. *Langmuir* **2008**, *24*, 7245.

(8) (a) Demessence, A.; D'Alessandro, D. M.; Foo, M. L.; Long, J. R. *J. Am. Chem. Soc.* **2009**, *131*, 8784. (b) An, J.; Geib, S. J.; Rosi, N. L. *J. Am. Chem. Soc.* **2010**, *132*, 38.

(9) (a) Caskey, S. R.; Wong-Foy, A. G.; Matzger, A. J. *J. Am. Chem. Soc.* **2008**, *130*, 10870. (b) Bloch, E. D.; Britt, D.; Lee, C.; Doonan, C. J.; Uribe-Romo, F. J.; Furukawa, H.; Long, J. R.; Yaghi, O. M. *J. Am. Chem. Soc.* **2010**, *132*, 14382. (c) Zhang, Z. J.; Xiang, S. C.; Hong, K. L.; Das, M. C.; Arman, H. D.; Garcia, M.; Mondal, J. U.; Thomas, K. M.; Chen, B. L. *Inorg. Chem.* **2012**, *51*, 4947.

(10) (a) Lin, J. B.; Zhang, J. P.; Chen, X. M. *J. Am. Chem. Soc.* **2010**, *132*, 6654. (b) Zhang, J. P.; Zhu, A. X.; Lin, R. B.; Qi, X. L.; Chen, X. M. *Adv. Mater.* **2011**, *23*, 1268. (c) Lin, Q. P.; Wu, T.; Zheng, S. T.; Bu, X. H.; Feng, P. Y. *J. Am. Chem. Soc.* **2012**, *134*, 784.

(11) Lässig, D.; Lincke, J.; Moellmer, J.; Reichenbach, C.; Moeller, A.; Gläser, R.; Kalies, G.; Cychosz, K. A.; Thommes, M.; Staudt, R.; Krautscheid, H. *Angew. Chem., Int. Ed.* **2011**, *50*, 10344.

(12) (a) Mammen, M.; Choi, S. K.; Whitesides, G. M. *Angew. Chem.* **1998**, *110*, 2908. (b) Dimmock, N. J. *Trends Biochem. Sci.* **1987**, *12*, 70.

(13) (a) Dincă, M.; Han, W. S.; Liu, Y.; Dailly, A.; Brown, C. M.; Long, J. R. *Angew. Chem., Int. Ed.* **2007**, *46*, 1419. (b) Li, J. R.; Tao, Y.; Yu, Q.; Bu, X. H.; Sakamoto, H.; Kitagawa, S. *Chem.—Eur. J.* **2008**, *14*, 2771. (c) Qin, J. S.; Du, D. Y.; Li, W. L.; Zhang, J. P.; Li, S. L.; Su, Z. M.; Wang, X. L.; Xu, Q.; Shao, K. Z.; Lan, Y. Q. *Chem. Sci* **2012**, *3*, 2114.

(14) Alkordi, M. H.; Brant, J. A.; Wojtas, L.; Kravtsov, V. Ch.; Cairns, A. J.; Eddaoudi, M. *J. Am. Chem. Soc.* **2009**, *131*, 17753.

(15) Spek, A. L. *J. Appl. Crystallogr.* **2003**, *36*, 7.

(16) (a) Park, K. S.; Ni, Z.; Côté, A. P.; Choi, J. Y.; Huang, R.; Uribe-Romo, F. J.; Chae, H. K.; O'Keeffe, M.; Yaghi, O. M. *Proc. Natl. Acad. Sci. U.S.A.* **2006**, *103*, 10186. (b) Hayashi, H.; Côté, A. P.; Furukawa, H.; O'Keefe, M.; Yaghi, O. M. *Nat. Mater.* **2007**, *6*, 501. (c) Sava, D. F.; Kravtsov, V. C.; Nouar, F.; Wojtas, L.; Eubank, J. F.; Eddaoudi, M. *J. Am. Chem. Soc.* **2008**, *130*, 3768.

(17) (a) Pachfule, P.; Chen, Y. F.; Sahoo, S. C.; Jiang, J. W.; Banerjee, R. *Chem. Mater.* **2011**, *23*, 2908. (b) Zhang, S. M.; Chang, Z.; Hu, T. L.; Bu, X. H. *Inorg. Chem.* **2010**, *49*, 11581.

(18) Lee, Y. G.; Moon, H. R.; Cheon, Y. E.; Suh, M. P. *Angew. Chem., Int. Ed.* **2008**, *47*, 7741.

(19) Si, X.; Jiao, C.; Li, F.; Zhang, J.; Wang, S.; Liu, S.; Li, Z.; Sun, L.; Xu, F.; Gabelica, Z.; Schick, C. *Energy Environ. Sci.* **2011**, *4*, 4522.

(20) Grimme, S. *J. Comput. Chem.* **2006**, *27*, 1787.